论著·基础研究

骨髓间充质干细胞来源小细胞外囊泡对骨质疏松症的改善作用

李旭冉[1,2,3]，陶诗聪[1,2,3#]，郭尚春[1,2,3#]

1. 上海交通大学医学院附属第六人民医院骨科，上海 200233；2. 上海交通大学医学院六院临床医学院，上海 200233；3. 上海交通大学医学院附属第六人民医院四肢显微外科研究所，上海 200233

［摘要］**目的**·探究人骨髓间充质干细胞（bone marrow mesenchymal stem cell，BMSC）来源的小细胞外囊泡（small extracellular vesicle，sEV）对小鼠破骨细胞分化和巨噬细胞极化的调控作用，以及对骨质疏松症小鼠的影响。**方法**·培养BMSC并通过差速离心法提取sEV，通过透射电子显微镜（transmission electron microscope，TEM）及纳米颗粒跟踪分析技术（nanoparticle tracking analysis，NTA）鉴定得到的sEV。通过巨噬细胞集落刺激因子（macrophage colony-stimulating factor，M-CSF）及核因子κB受体激活蛋白配体（receptor activator of nuclear factor-κB ligand，RANKL）刺激RAW264.7细胞以诱导形成破骨细胞，通过抗酒石酸酸性磷酸酶（tartrate-resistant acid phosphatase，TRAP）染色及鬼笔环肽染色检测sEV对破骨细胞分化的调控作用。通过荧光定量PCR检测sEV对破骨细胞标志基因环磷腺苷效应元件结合蛋白（cAMP-response element binding protein，*CREB*）、组织蛋白酶K（cathepsin K，*CTSK*）及*c-Jun*（Jun proto-oncogene）mRNA表达量的影响。使用脂多糖刺激RAW264.7细胞极化为M1型巨噬细胞；使用白细胞介素-4（interleukin-4，IL-4）及IL-13刺激RAW264.7细胞极化为M2型巨噬细胞。利用流式细胞术检测sEV对M1及M2型巨噬细胞极化的影响。通过微计算机断层扫描成像（micro-computed tomography，micro-CT）及TRAP染色观察sEV对骨质疏松症小鼠模型腰椎骨组织的影响。**结果**·TEM及NTA结果显示分离得到的sEV具有典型的球状结构，直径为30~150 nm。TRAP染色及鬼笔环肽染色结果显示，BMSC来源的sEV能够有效抑制RAW264.7细胞融合形成破骨细胞。PCR结果表明sEV能够降低*CREB*、*CTSK*和*c-Jun* mRNA的表达量（均$P<0.05$）。流式细胞术分析表明，BMSC来源的sEV能够抑制RAW264.7细胞极化为M1型巨噬细胞，促进其极化为M2型巨噬细胞。Micro-CT检测结果显示，sEV干预后模型小鼠腰椎骨小梁数量和骨体积分数显著高于未干预小鼠（均$P<0.05$）；TRAP染色结果显示，sEV干预后腰椎组织中的破骨细胞数量减少。**结论**·人BMSC来源的sEV可以延缓骨质疏松小鼠的骨质流失，这可能与其抑制小鼠破骨细胞分化及促进M2型巨噬细胞极化的作用有关。

［关键词］骨髓间充质干细胞；小细胞外囊泡；骨质疏松症；破骨细胞；巨噬细胞极化

［DOI］10.3969/j.issn.1674-8115.2023.04.002　［中图分类号］R681　［文献标志码］A

Ameliorative effects on osteoporosis of small extracellular vesicles derived from bone marrow mesenchymal stem cells

LI Xuran[1,2,3], TAO Shicong[1,2,3#], GUO Shangchun[1,2,3#]

1. Department of Orthopedic Surgery, Shanghai Sixth People's Hospital, Shanghai Jiao Tong University School of Medicine, Shanghai 200233, China; 2. Clinical Medical College of Shanghai Sixth People's Hospital, Shanghai Jiao Tong University School of Medicine, Shanghai 200233, China; 3. Institute of Microsurgery on Extremities, Shanghai Sixth People's Hospital, Shanghai Jiao Tong University School of Medicine, Shanghai 200233, China

[Abstract] **Objective**·To investigate the effects of small extracellular vesicles (sEVs) derived from human bone marrow mesenchymal stem cells (BMSCs) on the regulation of osteoclast differentiation and macrophage polarization in mice, and mouse model of osteoporosis. **Methods**·BMSCs were cultured and sEVs were isolated through differential centrifugation. The isolated

[基金项目] 国家自然科学基金（81802226，81871834，82072530）；上海市浦江人才计划（2019PJD038）；2020年上海市“医苑新星”青年医学人才培养资助计划；上海市第六人民医院优秀人才培育项目（ynyq202101）；上海交通大学医学院“双百人”项目（2022-017）。

[作者简介] 李旭冉（1999—），男，硕士生；电子信箱：15737905921@163.com。

[通信作者] 郭尚春，电子信箱：scguo@shsmu.edu.cn。陶诗聪，电子信箱：sctao@shsmu.edu.cn。#为共同通信作者。

[Funding Information] National Natural Science Foundation of China (81802226, 81871834, 82072530); Shanghai Pujiang Program (2019PJD038); Shanghai “Rising Stars of Medical Talent” Youth Development Program in 2020; Shanghai Sixth People's Hospital Funding (ynyq202101); "Two-hundred Talents" Program of Shanghai Jiao Tong University School of Medicine (2022-017).

[Corresponding Author] GUO Shangchun, E-mail: scguo@shsmu.edu.cn. TAO Shicong, E-mail: sctao@shsmu.edu.cn. #Co-corresponding authors.

sEVs were identified by transmission electron microscopy (TEM) and nanoparticle tracking analysis (NTA). RAW264.7 cells were cultured and stimulated with macrophage colony-stimulating factor (M-CSF) and receptor activator of nuclear factor-κB ligand (RANKL) to differentiate the cells into osteoclasts. Tartrate-resistant acid phosphatase (TRAP) staining and phalloidin staining were performed to assess the effect of sEVs on osteoclast formation. The expression levels of osteoclast marker genes, *i.e.*, cAMP-response element binding protein (*CREB*), cathepsin K (*CTSK*), and Jun proto-oncogene (*c-Jun*) were examined by real-time quantitative PCR. To polarize RAW264.7 cells to M1 phenotype, they were cultured with lipopolysaccharides; to polarize them to M2 phenotype, they were cultured with interleukin-4 (IL-4) and IL-13. Flow cytometry was performed to detect the effect of sEVs on macrophage polarization. Micro-computed tomography (micro-CT) and TRAP staining were performed to investigate the effect of sEVs on the bone tissues of lumbar vertebrae in osteoporosis mouse models. **Results**·TEM and NTA demonstrated that the isolated sEVs had a typical globular structure with a diameter ranging from 30–150 nm. TRAP staining and phalloidin staining showed that BMSC-derived sEVs inhibited the fusion of RAW264.7 cells to form osteoblasts. PCR revealed that sEVs could decrease the expression of *CREB*, *CTSK*, and *c-Jun* (all $P<0.05$). Flow cytometry analysis indicated that BMSC-derived sEVs inhibited RAW264.7 macrophages polarization to M1 phenotype and induced RAW264.7 macrophages polarization to M2 phenotype. Micro-CT indicated that the number of trabeculae and the bone volume fraction of lumbar vertebrae were significantly higher in the sEV-intervened group than those in the control group (both $P<0.05$). TRAP staining revealed a reduction of osteoclast number in the lumbar vertebrae after intervention with sEVs. **Conclusion**·The sEVs from human BMSCs can delay bone loss in osteoporosis mice, which may be related to its effects of inhibiting osteoclast differentiation and promoting the polarization of M2 type macrophages.

[Key words] bone marrow mesenchymal stem cell (BMSC); small extracellular vesicle (sEV); osteoporosis; osteoclast; macrophage polarization

骨质疏松症（osteoporosis）是一种全身性、代谢性疾病，其特征为骨组织微结构退化，骨量减少，进而导致骨骼强度降低、脆性增加[1]。我国骨质疏松症患者基数较大，且随着老龄化程度增加，患病率及骨质疏松性骨折发生率也逐渐提高，给患者家庭及社会造成负担[2-3]。

骨代谢稳态是骨吸收与骨形成的动态平衡过程，这与成骨细胞、破骨细胞及巨噬细胞等细胞的功能密切相关[4-5]。当骨吸收作用增强时，骨稳态失衡，骨质流失，严重时可导致骨质疏松症[6]。破骨细胞具有骨吸收的功能，可通过分泌酸和蛋白酶等吸收骨质，在骨发育与骨重塑中有着重要作用[7]。破骨细胞活性减弱可导致石骨症，过度活跃时可导致骨质疏松症[8]。核因子κB受体激活蛋白配体（receptor activator of nuclear factor-κB ligand，RANKL）是调节破骨细胞活性的重要因子，骨细胞可通过分泌RANKL促进破骨细胞分化，从而维持骨形成与骨吸收的动态平衡[9-10]。此外，其他细胞因子也可调节破骨细胞分化，增强破骨细胞活性，进而导致骨质流失[7,11-12]。

巨噬细胞参与固有免疫反应，在骨稳态中也有着重要作用[13]。巨噬细胞可极化为不同的表型，主要分为2种亚型：具有促炎作用的M1型及具有抗炎作用的M2型[14]。M1型巨噬细胞可分泌促炎细胞因子，如肿瘤坏死因子-α（tumor necrosis factor-α，TNF-α）、白细胞介素-6（interleukin-6，IL-6）及IL-8等[15]；M2型巨噬细胞可分泌多种抗炎细胞因子，如IL-10、血管内皮生长因子（vascular endothelial growth factor，VEGF）及转化生长因子-β（transforming growth factor-β，TGF-β）等，可抑制炎症并促进组织修复[16-17]。M1/M2比例失衡与骨质疏松症密切相关：M1型巨噬细胞可通过分泌细胞因子诱导破骨细胞分化，激活骨吸收，从而加剧骨质流失[18-19]；M2型巨噬细胞可以诱导干细胞向成骨细胞分化，从而促进骨形成[20]。调控巨噬细胞极化是维持骨稳态、改善骨质疏松症的潜在方法[21]。

小细胞外囊泡（small extracellular vesicle，sEV）是一类起源于细胞多泡体的双层囊泡，通过细胞胞吐作用释放[21]。几乎所有人体细胞都可产生sEV。研究[22]表明，sEV中包含大量脂质、蛋白质及RNA等生物大分子，在细胞间通信中有重要作用。此外，sEV具有调控细胞增殖、迁移及分化等多种功能[23-25]。研究[26-27]表明，sEV可通过携带的RNA影响成骨相关转录因子的表达，促进干细胞向成骨细胞分化，并抑制骨髓间充质干细胞（bone marrow mesenchymal stem cell，BMSC）向脂肪细胞分化；但sEV能否通过调控破骨细胞分化及巨噬细胞极化从而改善骨质疏松症，仍有待进一步阐明。

本研究提取BMSC来源的sEV，通过细胞实验探索sEV对破骨细胞分化及巨噬细胞极化的调控作用，并通过体内实验探索sEV对骨质疏松症潜在的治疗作用。

1 材料与方法

1.1 实验材料

1.1.1 实验细胞及动物 小鼠巨噬细胞RAW264.7购于中国科学院细胞库。人BMSC（HUXMA-01001）购于中国赛业生物科技有限公司。8周龄健康雌性C57BL/6J小鼠购于上海市计划生育科学研究所实验动物经营部，实验动物生产许可证号为SCXK（沪）2018-0006；小鼠饲养于上海交通大学医学院附属第六人民医院动物实验室，实验动物使用许可证号为SYXK（沪）2016-0020。

1.1.2 主要试剂和仪器 胎牛血清（fetal bovine serum，FBS；货号FBSSR-01021，中国赛业），MEM细胞培养基（货号10370-070；美国Gibco），脂多糖（lipopolysaccharides，LPS；货号L2880，美国Sigma-Aldrich），抗酒石酸酸性磷酸酶（tartrate-resistant acid phosphatase，TRAP）染色试剂盒（货号PMC-AK04F-COS，日本Wako），巨噬细胞集落刺激因子（macrophage colony-stimulating factor，M-CSF；货号CB34，中国近岸蛋白质），IL-4（货号CK15，中国近岸蛋白质）；IL-13（货号CH18，中国近岸蛋白质），RANKL（货号CJ94，中国近岸蛋白质），BB700标记的大鼠抗小鼠CD86抗体（货号742120，美国BD Pharmingen），APC标记的抗小鼠巨噬细胞甘露糖受体（macrophage mannose receptor，MMR，又称CD206）抗体（货号FAB2535A，美国R&D Systems），iFluor™ 488标记鬼笔环肽试剂（货号40736ES75，中国翌圣），抗荧光衰减封片剂（含细胞核染料DAPI；货号S2110，中国索莱宝），总RNA提取试剂（TRIzol；货号R1100，中国索莱宝），反转录试剂盒（货号11123ES60，中国翌圣），实时荧光定量PCR扩增预混合液（qPCR SYBR Green Master Mix；货号11204ES08，中国翌圣），PCR引物（中国BioTNT公司），外泌体荧光标记染料（DiR；货号UR21017，中国宇玫博）。

倒置荧光显微镜（Eclipse Ts2R-FL，日本Nikon），微计算机断层扫描成像系统（micro-computed tomography，micro-CT；Skyscan 1176，德国Bruker），流式细胞仪（CytoFLEX system，美国Beckman Coulter），透射电子显微镜（transmission electron microscopy，TEM；JEM 2100F，日本JEOL），纳米颗粒跟踪分析仪（NanoSight NS300，英国Malvern Panalytical），荧光定量PCR仪（LightCycler®480 Ⅱ，瑞士Roche），小动物活体成像系统（VISQUE InVivo ART，韩国Vieworks）。

1.2 实验方法

1.2.1 sEV的分离与鉴定 培养BMSC并在细胞融合度达到80%~90%时，收集细胞培养液。为去除细胞及细胞碎片，分别以300×*g*、2 000×*g*及10 000×*g*离心10 min、10 min及30 min，收集上清液并用孔径0.22 μm滤器过滤。将过滤后的上清液以100 000×*g*离心70 min，收集sEV，用无菌PBS溶液重悬sEV并储存备用。所有离心均在4 ℃中进行。获得的sEV部分用于鉴定、细胞培养及动物实验，余下的部分置于−80 ℃冰箱保存。按照TEM及纳米颗粒跟踪分析（nanoparticle tracking analysis，NTA）制样要求稀释sEV，稀释后上机检测。

1.2.2 破骨细胞的诱导培养 分别按照7.5×10^5个/孔及1.5×10^6个/孔的密度将RAW264.7细胞接种于6孔细胞培养板中；配置含有30 ng/mL M-CSF及100 ng/mL RANKL的破骨细胞诱导培养基进行细胞诱导和培养，隔天换液，观察细胞形态并在第1、第5、第8日拍照。选择合适的细胞接种密度，并分为对照组及sEV组，均以破骨细胞诱导培养基培养，sEV组的培养基中加入sEV，浓度为2×10^{10}个/mL。

1.2.3 TRAP染色 按试剂盒说明书操作。在培养板中观察到融合的破骨细胞后，用多聚甲醛固定液固定细胞并清洗。将去离子水预热到37 ℃，配置酒石酸盐缓冲液，并加入培养板中。之后在培养板中加入显色底物，避光水浴孵育2 h。使用去离子水清洗培养板，在倒置显微镜下拍照。

1.2.4 鬼笔环肽染色 使用多聚甲醛溶液在室温条件下固定细胞10 min，并用PBS清洗。配置鬼笔环肽工作液，在培养板中加入适量染液，室温避光染色2 h，并用PBS清洗。配置DAPI工作液，并加入培养板中，室温避光染色10 min，在显微镜下观察实验结果。

1.2.5 实时荧光定量PCR 使用TRIzol试剂提取细胞总RNA，并将得到的总RNA稀释至适宜浓度，按照说明书进行反转录得到cDNA溶液，将适量cDNA溶液与SYBR Green Mix试剂、引物溶液及蒸馏水等混合以配置PCR工作体系，在荧光定量PCR仪中进行检测。PCR反应条件为：预变性95 ℃ 5 min；变性95 ℃ 10 s，退火及延伸60 ℃ 30 s，共计40个循环。引物序列详见表1。

表1　荧光定量PCR引物序列

Tab 1　Primer sequences for qPCR

Primer	Sequence
β-actin forward	5′-CCTCTATGCCAACACAGT-3′
β-actin reverse	5′-AGCCACCAATCCACACAG-3′
CREB forward	5′-CCTTGCTTTCCGAATCCTC-3′
CREB reverse	5′-CACTTTGGCTGGACATCTTG-3′
c-Jun forward	5′-AGCAACTTTCCTGACCCAGAG-3′
c-Jun reverse	5′-TCTTTACAGTCTCGGTGGCAG-3′
CTSK forward	5′-CCAGAATCTTGTGGACTGTGT-3′
CTSK reverse	5′-CATCTTCAGAGTCAATGCCTC-3′

Note: *CREB*—cAMP-response element binding protein; *c-Jun*—Jun proto-oncogene; *CTSK*—cathepsin K.

1.2.6　诱导巨噬细胞极化　在6孔板中按照5×10^5个/孔接种RAW264.7细胞，并分为空白组、对照组及sEV组（M1型巨噬细胞极化为空白组$_1$、对照组$_1$及sEV组$_1$；M2型巨噬细胞极化为空白组$_2$、对照组$_2$及sEV组$_2$）。诱导M1型巨噬细胞极化：空白组$_1$使用MEM细胞培养液培养2 d，对照组$_1$使用含有200 ng/mL LPS的细胞培养液诱导2 d，sEV组$_1$使用含有200 ng/mL LPS和2×10^{10}个/mL sEV的培养液诱导2 d，3组细胞均24 h换液1次。诱导M2型巨噬细胞极化：空白组$_2$使用MEM细胞培养液培养2 d，对照组$_2$使用含有40 ng/mL IL-4及40 ng/mL IL-13的细胞培养液诱导2 d，sEV组$_2$在对照组$_2$培养液的基础上再添加2×10^{10}个/mL sEV诱导2 d，3组细胞均24 h换液1次。

1.2.7　流式细胞分析　巨噬细胞极化诱导结束后，分别收集空白组$_{1/2}$、对照组$_{1/2}$及sEV组$_{1/2}$的RAW264.7细胞，以300×*g*离心5 min，用PBS重悬以清洗细胞。室温下用多聚甲醛溶液固定10 min，并用PBS清洗。使用含有5% FBS的封闭液室温孵育10 min，PBS清洗并弃上清液。按照说明书分别配置CD86抗体（M1型巨噬细胞极化组）及CD206抗体（M2型巨噬细胞极化组）工作液，重悬细胞，室温下避光孵育30 min。孵育结束后，使用PBS重悬细胞，用流式细胞仪进行检测。

1.2.8　小动物活体成像　使用PBS配置DiR染料工作液。在sEV中加入适量DiR工作液，通过涡旋振荡器混匀并在水浴锅中孵育30 min，利用超速离心法去除多余染料，最后用PBS重悬。将C57BL/6J小鼠分为对照组及sEV组，sEV组小鼠通过尾静脉注射DiR标记的sEV（2×10^{10}个/mL），对照组小鼠注射等量PBS。24 h后，取2组小鼠的股骨、胫骨及脊柱，使用小动物活体成像系统观察小鼠骨骼内sEV的分布情况。

1.2.9　骨质疏松症动物模型　取8周龄的雌性C57BL/6J小鼠，去除双侧卵巢（ovariectomized，OVX）以建立骨质疏松症动物模型，并分为OVX组和OVX+sEV组。自第2周起，OVX+sEV组小鼠每2周通过尾静脉注射500 μL的2×10^{10}个/mL sEV溶液1次，OVX组通过尾静脉注射等量生理盐水。12周后处死小鼠并取腰椎组织。固定腰椎组织并进行micro-CT扫描，分析骨体积分数（bone volume/tissue volume，BV/TV）及骨小梁数量（trabecular number，Tb.N）。将腰椎组织进行脱钙处理，使用乙醇脱水并利用二甲苯透明，浸蜡包埋腰椎组织并切片，按照说明书进行TRAP染色。

1.3　统计学分析

采用GraphPad Prism 9.0进行统计学分析并绘图。定量资料用$\bar{x}\pm s$表示，2组间比较采用*t*检验。$P<0.05$表示差异具有统计学意义。

2　结果

2.1　sEV的分离与表征

通过差速离心法得到sEV，并利用TEM及NTA对得到的sEV进行鉴定。TEM结果显示，sEV具有典型的球状结构，其直径为30~150 nm（图1A）。NTA结果显示，大部分sEV直径在52~116 nm之间，证明BMSC来源的sEV具有较好的均一性（图1B）。

2.2　破骨细胞诱导与预实验

在6孔细胞培养板中分别按7.5×10^5个/孔和1.5×10^6个/孔的密度接种RAW264.7细胞，并诱导为破骨细胞。通过显微镜观察不同时间点下细胞的形态与融合状态。结果表明，接种密度较高时（1.5×10^6个/孔），8 d内并未观测到具有多个细胞核的典型破骨细胞（图2A）；接种密度较低时（7.5×10^5个/孔），RAW264.7细胞在第5日时产生了多细胞融合的破骨细胞，在第8日时产生了更多具有典型形态的破骨细胞，并能在破骨细胞内观测到更多的细胞核（图2B）。TRAP染色结果显示，在较高密度下的RAW264.7细胞并未观测到具有紫红色胞浆的多核破骨细胞（图2C）；较低密度下的RAW264.7细胞融合形成了多个破骨细胞，且破骨细胞形态典型，胞浆呈现明显的紫红色（图2D）。因此后续破骨细胞诱导实验采用较低密度（7.5×10^5个/孔）种板。

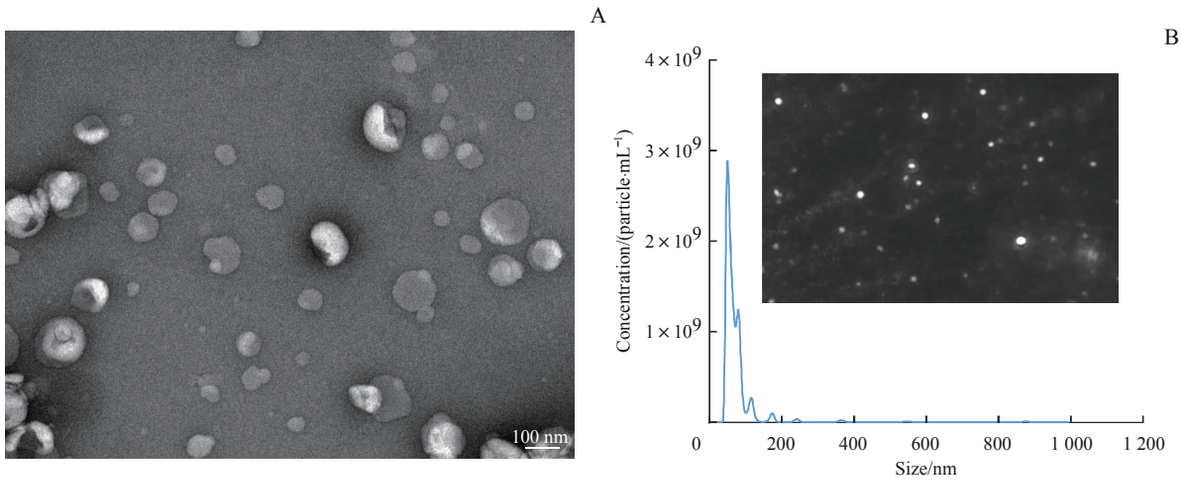

Note: A. The typical morphology of sEVs in a TEM image (×20 000). B. The result and a typical image of NTA.

图1 通过TEM及NTA对BMSC来源sEV的鉴定

Fig 1 Identification of sEVs from BMSCs by TEM and NTA

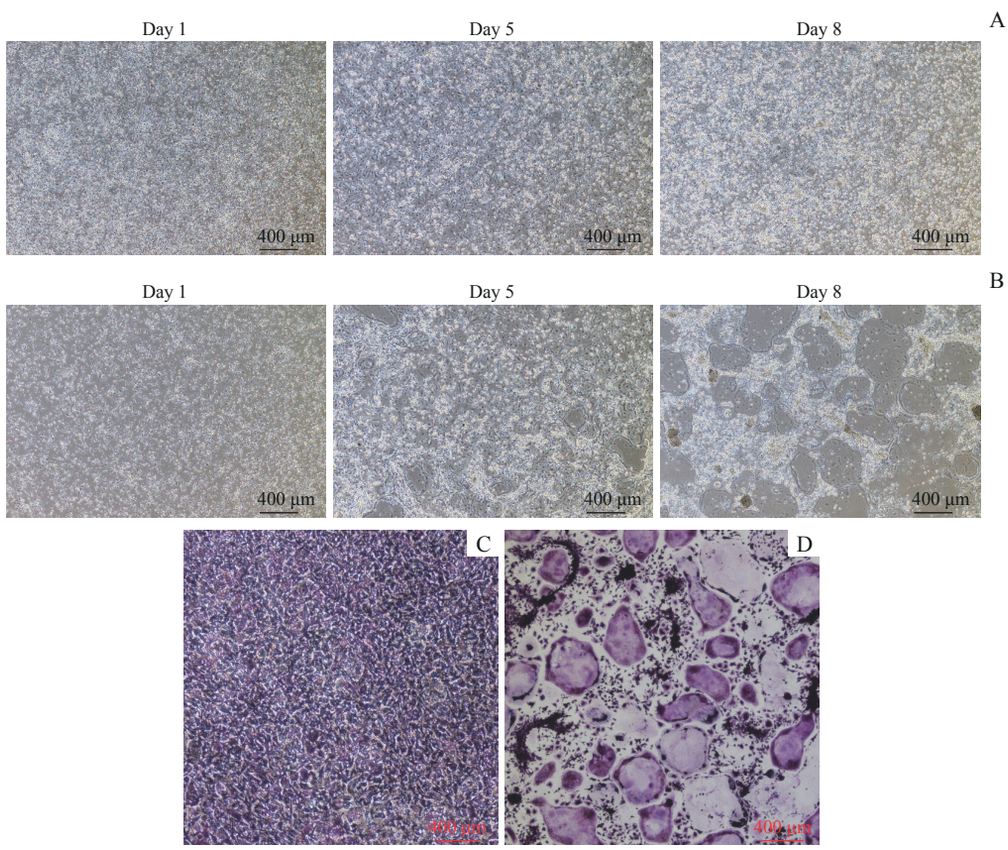

Note: A/B. The RAW264.7 cells were seeded at a high density (1.5×10^6 per well, A) and a low density (7.5×10^5 per well, B) and the formation of osteoclasts was observed at different time-points (×40). C/D. The results of TRAP staining of the cells seeded at a high density (C) and a low density (D) (×40).

图2 诱导破骨细胞分化及TRAP染色结果

Fig 2 Formation of osteoclasts and the results of TRAP staining

2.3 sEV调控破骨细胞分化

诱导RAW264.7细胞向破骨细胞分化，并分为对照组和sEV组。在第8日进行TRAP染色及鬼笔环肽染色。TRAP染色结果显示，对照组中形成了大量破骨细胞，胞体较大；sEV组中形成的多核破骨细胞数量较少，胞体较小（图3）。鬼笔环肽染色结果同样显示，对照组形成了较多的破骨细胞，形态典型且胞体较大，sEV组中典型的破骨细胞较少，胞体较小（图4）。说明BMSC来源的sEV可以抑制RAW264.7细胞向破骨细胞分化。

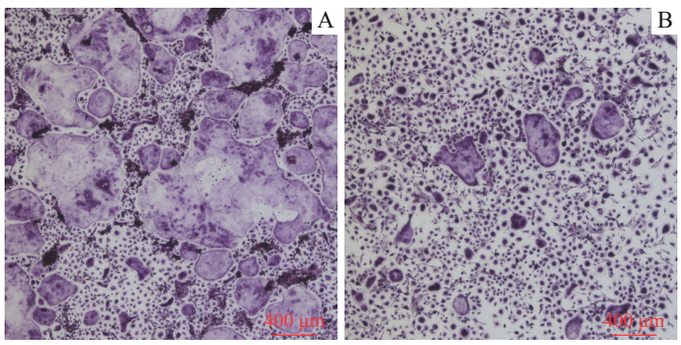

Note：A. The control group. B. The sEV group.

图3　2组细胞向破骨细胞分化后的TRAP染色结果 (×40)

Fig 3　TRAP staining results of two groups of cells differentiated into osteoclasts (×40)

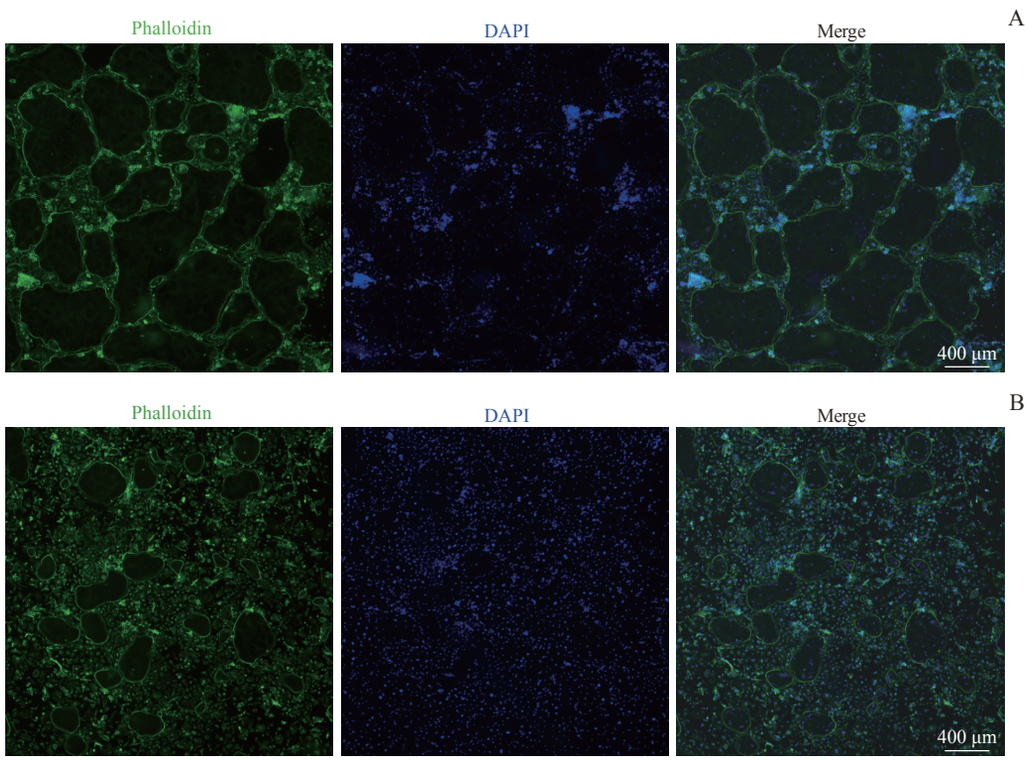

Note：A. The control group. B. The sEV group.

图4　2组细胞向破骨细胞分化后的鬼笔环肽染色结果 (×40)

Fig 4　Phalloidin staining results of two groups of cells differentiated into osteoclasts (×40)

CTSK、*CREB*及*c-Jun*是破骨细胞特异性标志表达基因[28-30]。实时荧光定量PCR检测结果（图5）显示，sEV组的*CREB* mRNA表达量是对照组的（80.6±6.4）%，*CTSK* mRNA表达量为对照组的（34.2±0.9）%，*c-Jun* mRNA表达量是对照组的（37.3±0.8）%，差异均具有统计学意义（均P<0.05）。结果说明，sEV可以抑制破骨细胞分化及成熟相关基因的表达。

2.4　sEV调控巨噬细胞极化

将RAW264.7细胞分别诱导为M1型及M2型巨噬细胞。经流式细胞术检测发现：以空白组$_1$作为参照，M1型巨噬细胞标志物CD86在对照组$_1$中高表达（67.0%），在sEV组$_1$中表达明显下降（14.3%，图6）；M2型巨噬细胞标志物CD206在对照组$_2$中低表达（51.0%），在sEV组$_2$中表达高表达（70.1%，图7）。结果说明，sEV可以抑制RAW264.7细胞向M1型巨噬细胞极化，促进其向M2型巨噬细胞极化。

2.5　sEV延缓小鼠骨质疏松模型骨质流失

利用荧光染料DiR标记sEV，尾静脉注射后24 h取小鼠部分骨骼，并利用小动物活体成像系统检测sEV分布情况。成像结果（图8）显示，sEV组小鼠

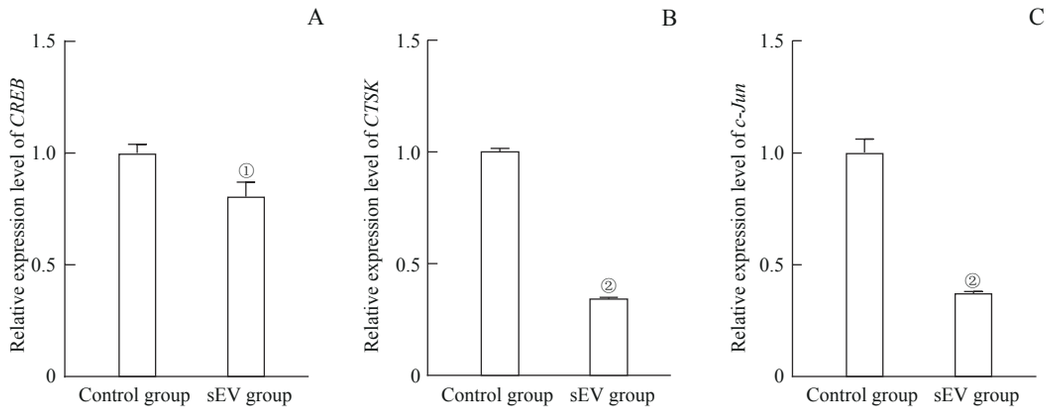

Note: ①P=0.011, ②P=0.000, compared with the control group.

图5 荧光定量PCR检测2组细胞向破骨细胞分化后的*CREB* (A)、*CTSK* (B)与*c-Jun* (C)的mRNA水平

Fig 5 mRNA levels of *CREB* (A), *CTSK* (B) and *c-Jun* (C) detected by qPCR after the cells differentiated into osteoclasts in the two groups

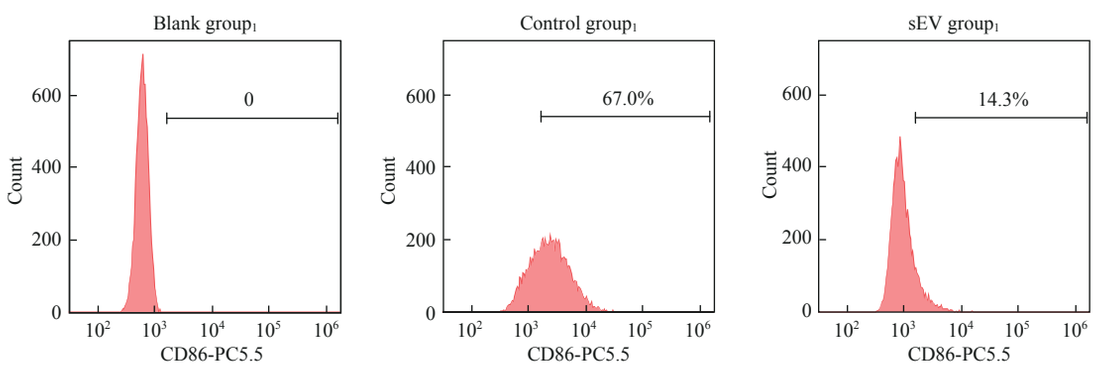

图6 流式细胞术检测M1型巨噬细胞标志物（CD86）表达水平

Fig 6 Expression level of M1 macrophage marker (CD86) detected by flow cytometry

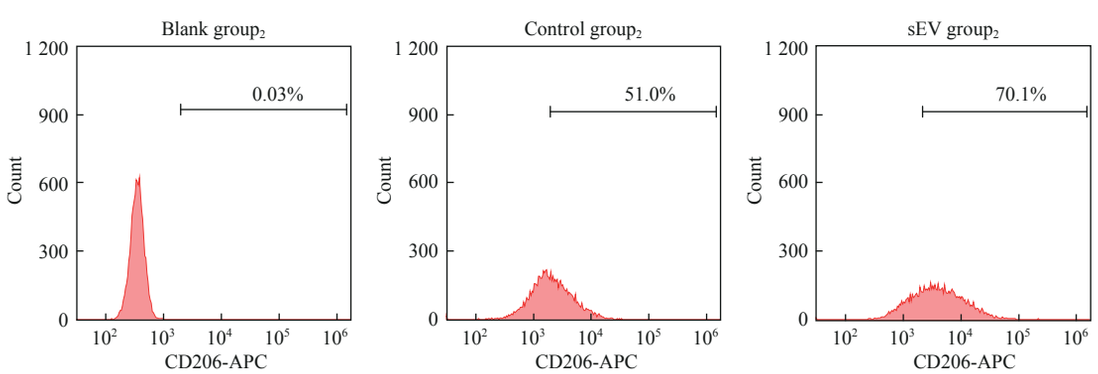

图7 流式细胞术检测M2型巨噬细胞标志物（CD206）表达水平

Fig 7 Expression level of M2 macrophage marker (CD206) detected by flow cytometry

脊柱及下肢骨骼中存在DiR标记的sEV，表明sEV可以被小鼠骨髓摄取。

建立骨质疏松症小鼠模型，12周后取腰椎并利用micro-CT分析。结果表明，相比OVX组，OVX+sEV组腰椎骨质流失不明显，骨小梁数量较OVX组多，骨体积分数相对较高（图9）。TRAP染色结果（图10）发现，OVX组腰椎组织中存在大量破骨细胞，且破骨细胞分布均匀；而OVX+sEV组的破骨细胞数量较少，呈零星分布。结果表明sEV抑制了骨质疏松症小鼠模型的骨质流失，减少了骨组织中的破骨细胞数量。

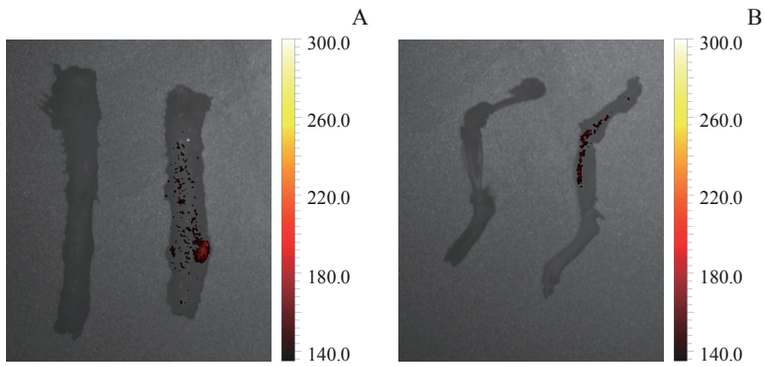

Note：A. The live imaging of the spines (left: the control group; right: the sEV group). B. The live imaging of the femurs and the tibias (left: the control group; right: the sEV group).

图8　活体成像观察小鼠骨骼中sEV分布情况

Fig 8　Observation of sEVs distribution in mouse bones by living imaging

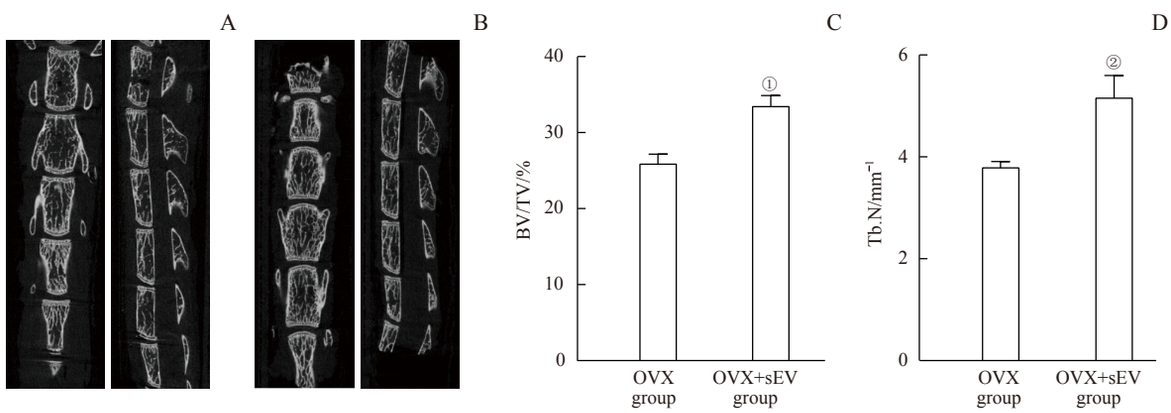

Note：A. The lumbar spine of the OVX group. B. The lumbar spine of the OVX+sEV group. C. The BV/TV values of 2 groups. D. The Tb.N values of 2 groups. ①P=0.002, ②P=0.005, compared with the OVX group.

图9　骨质疏松症小鼠及sEV干预小鼠的micro-CT影像学分析及骨参数

Fig 9　Micro-CT imaging analysis and bone parameters of the osteoporosis mice and the sEV-intervened mice

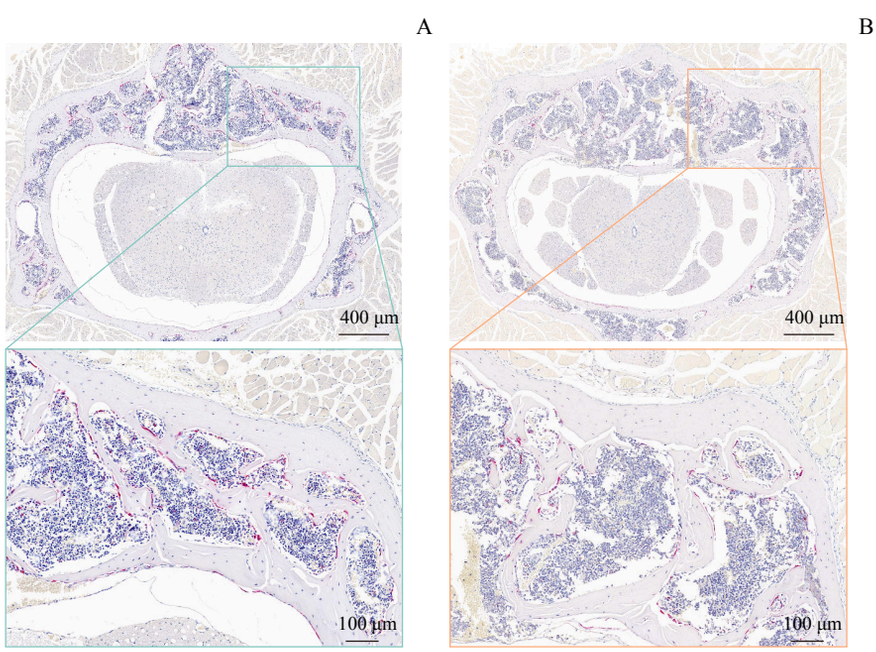

Note：A. The OVX group. B. The OVX+sEV group. Above (×5); below (×30).

图10　骨质疏松症小鼠及sEV干预小鼠腰椎的TRAP染色结果

Fig 10　TRAP staining images of the osteoporosis mice and the sEV-intervened mice

3 讨论

研究[31]表明，sEV的直径为30~150 nm，包含脂质双层、蛋白质及核酸等物质。我们通过差速离心法得到了BMSC来源的sEV，通过TEM及NTA技术验证了BMSC来源的sEV直径介于30~150 nm。近年来sEV提取纯化方法也得到了发展。差速离心法是提取sEV的经典方法，密度梯度离心法是在差速离心法的基础上，利用蔗糖密度梯度进一步纯化sEV[32]。目前已开发出商业化的sEV提取试剂盒，提高了sEV的提取效率。与差速离心法等相比，经试剂盒提取的sEV纯度更高，促进了sEV的产业化发展[33-34]。

多种因素可导致骨代谢稳态紊乱，骨皮质厚度减少，骨小梁变薄甚至丢失，进而导致骨质疏松症[35]。破骨细胞在骨质疏松症的形成与发展中有重要作用。胆固醇代谢过程中产生的27-羟基胆固醇可竞争性结合雌激素受体并促进破骨细胞分化，导致骨质流失[36-37]。微RNA（miRNA）是调控基因表达的重要因子，部分miRNA与骨质疏松症的发病机制密切相关，如miR-483-5p可通过靶向胰岛素样生长因子-2促进破骨细胞分化，导致骨质流失[38]。甲基乙二醛可通过c-Jun氨基末端蛋白激酶信号通路激活破骨细胞，从而导致骨质疏松症[6]。抑制破骨细胞分化是治疗骨质疏松症的重要方法，如落干酸可通过抑制破骨细胞分化避免骨密度下降，改善骨骼微结构[39]。我们的实验证明了BMSC来源的sEV可以抑制破骨细胞分化，具有抑制骨吸收的作用。研究表明sEV中的RNA对破骨细胞的形成具有调控作用。LAI等[40]发现BMSC来源的sEV中含有miR-27a-3p和miR-196b-5p，可促进干细胞的成骨分化并抑制破骨细胞的形成。SONG等[41]证明内皮细胞来源的sEV通过miR-155抑制巨噬细胞形成破骨细胞，具有治疗骨质疏松症的潜力。研究[42]发现，M2型巨噬细胞来源的sEV可通过递送IL-10相关的mRNA激活IL-10下游信号通路，抑制破骨细胞的形成。

骨髓巨噬细胞在骨稳态调节中有重要作用。M1型巨噬细胞可以促进破骨细胞分化并抑制成骨细胞活性，从而抑制成骨[43-44]。M2型巨噬细胞可以诱导干细胞向成骨细胞分化以促进成骨[45]。此外，M2型巨噬细胞分泌的抗炎细胞因子及趋化因子等可以促进骨重塑[46-47]。调控巨噬细胞极化是治疗骨质疏松症的潜在方法，抑制巨噬细胞向M1型极化可预防骨质疏松症[48]。抑制核因子-κB以及丝裂原活化蛋白激酶信号通路可以促进巨噬细胞向M2型极化并抑制破骨细胞生成，从而延缓骨质流失[49]。我们发现BMSC来源的sEV可以抑制破骨细胞分化并促进巨噬细胞向M2型极化。已有的研究[50-51]表明，sEV可通过miRNA促进巨噬细胞向M2型极化。脂肪干细胞来源的sEV通过miR-451a调控M2型巨噬细胞极化从而促进骨愈合[52]。BMSC来源的sEV可下调内质网到细胞核信号转导蛋白1（endoplasmic reticulum to nucleus signaling 1，ERN1）的表达促进M2型巨噬细胞极化[53]。

破骨细胞增多及M1型巨噬细胞增多是骨代谢失衡的影响因素[5,18]。本研究通过体内外实验证明了人BMSC来源的sEV具有抑制小鼠破骨细胞分化及促进M2型巨噬细胞极化的能力，对骨质疏松症小鼠模型骨质流失有一定的改善作用。此外，sEV具有较好的生物相容性，无免疫原性，临床应用前景广阔，为骨质疏松症的治疗提供了新的策略。

利益冲突声明/Conflict of Interests

所有作者声明不存在利益冲突。

All authors disclose no relevant conflict of interests.

伦理批准和动物权利声明/Ethics Approval and Animal Right

本研究涉及的动物实验均已通过上海交通大学医学院附属第六人民医院动物福利委员会的批准（批准号2021-0767）。所有实验均遵照上海交通大学医学院第六人民医院动物实验室制定的实验动物操作标准进行。

All animal experiments were approved by the Animal Welfare Committee of Shanghai Sixth People's Hospital, Shanghai Jiao Tong University School of Medicine (Grant No. 2021-0767). All experimental manipulations were performed following the guidelines of the animal laboratory of Shanghai Sixth People's Hospital, Shanghai Jiao Tong University School of Medicine.

作者贡献/Authors' Contributions

郭尚春、陶诗聪负责课题设计及论文的修改。李旭冉负责实验操作、数据分析和论文写作。所有作者均阅读并同意了最终稿件的提交。

GUO Shangchun and TAO Shicong were responsible for experimental design and paper revising. LI Xuran was responsible for experiments, data analyses, and paper writing. All the authors have read the last version of paper and consented for submission.

· Received: 2022-12-23
· Accepted: 2023-03-27
· Published online: 2023-04-28

参·考·文·献

[1] CHEATHAM S W, HANNEY W, KOLBER M, et al. Osteoporosis: exercise programming insight for the sports medicine professional[J]. Strength Cond J, 2017, 39: 2-13.

[2] SI L, WINZENBERG T M, JIANG Q, et al. Projection of osteoporosis-related fractures and costs in China: 2010 – 2050[J]. Osteoporos Int, 2015, 26(7): 1929-1937.

[3] YU F, XIA W B. The epidemiology of osteoporosis, associated fragility fractures, and management gap in China[J]. Arch Osteoporos, 2019, 14(1): 32.

[4] LEE C W, LIN H C, WANG B Y, et al. Ginkgolide B monotherapy reverses osteoporosis by regulating oxidative stress-mediated bone homeostasis[J]. Free Radic Biol Med, 2021, 168: 234-246.

[5] LIU P, LEE S, KNOLL J, et al. Loss of menin in osteoblast lineage affects osteocyte-osteoclast crosstalk causing osteoporosis[J]. Cell Death Differ, 2017, 24(4): 672-682.

[6] LEE K M, LEE C Y, ZHANG G, et al. Methylglyoxal activates osteoclasts through JNK pathway leading to osteoporosis[J]. Chem Biol Interact, 2019, 308: 147-154.

[7] BARSONY J, XU Q, VERBALIS J G. Hyponatremia elicits gene expression changes driving osteoclast differentiation and functions[J]. Mol Cell Endocrinol, 2022, 554: 111724.

[8] JACOME-GALARZA C E, PERCIN G I, MULLER J T, et al. Developmental origin, functional maintenance and genetic rescue of osteoclasts[J]. Nature, 2019, 568(7753): 541-545.

[9] PESCE VIGLIETTI A I, GIAMBARTOLOMEI G H, DELPINO M V. Endocrine modulation of *Brucella abortus*-infected osteocytes function and osteoclastogenesis *via* modulation of RANKL/OPG[J]. Microbes Infect, 2019, 21(7): 287-295.

[10] KIM J M, LIN C J, STAVRE Z, et al. Osteoblast-osteoclast communication and bone homeostasis[J]. Cells, 2020, 9(9): 2073.

[11] QIAN J, HE Y, ZHAO J, et al. IL4/IL4R signaling promotes the osteolysis in metastatic bone of CRC through regulating the proliferation of osteoclast precursors[J]. Mol Med, 2021, 27(1): 152.

[12] YAO Z, GETTING S J, LOCKE I C. Regulation of TNF-induced osteoclast differentiation[J]. Cells, 2021, 11(1): 132.

[13] KANG M Y, HUANG C C, LU Y, et al. Bone regeneration is mediated by macrophage extracellular vesicles[J]. Bone, 2020, 141: 115627.

[14] CAI F Y, LIU S L, LEI Y X, et al. Epigallocatechin-3 gallate regulates macrophage subtypes and immunometabolism to ameliorate experimental autoimmune encephalomyelitis[J]. Cell Immunol, 2021, 368: 104421.

[15] ZHANG Z G, ZHANG C Y, ZHANG S R. Irisin activates M1 macrophage and suppresses Th2-type immune response in rats with pelvic inflammatory disease[J]. Evid Based Complement Alternat Med, 2022, 2022: 5215915.

[16] EOM J, YOO J, KIM J J, et al. Viperin deficiency promotes polarization of macrophages and secretion of M1 and M2 cytokines[J]. Immune Netw, 2018, 18(4): e32.

[17] ZHANG W J, GUAN N, ZHANG X M, et al. Study on the imbalance of M1/M2 macrophage polarization in severe chronic periodontitis[J]. Technol Health Care, 2023, 31(1): 117-124.

[18] WANG W H, LIU H, LIU T, et al. Insights into the role of macrophage polarization in the pathogenesis of osteoporosis[J]. Oxid Med Cell Longev, 2022, 2022: 2485959.

[19] YU L, HU M, CUI X, et al. M1 macrophage-derived exosomes aggravate bone loss in postmenopausal osteoporosis *via* a microRNA-98/DUSP1/JNK axis[J]. Cell Biol Int, 2021, 45(12): 2452-2463.

[20] LU Y P, LIU S S, YANG P P, et al. Exendin-4 and eldecalcitol synergistically promote osteogenic differentiation of bone marrow mesenchymal stem cells through M2 macrophages polarization *via* PI3K/AKT pathway[J]. Stem Cell Res Ther, 2022, 13(1): 113.

[21] CHEN M, LIN W M, YE R, et al. PPARβ/δ agonist alleviates diabetic osteoporosis *via* regulating M1/M2 macrophage polarization[J]. Front Cell Dev Biol, 2021, 9: 753194.

[22] WEI H, CHEN Q, LIN L, et al. Regulation of exosome production and cargo sorting[J]. Int J Biol Sci, 2021, 17(1): 163-177.

[23] LI M D, JIA J, LI S S, et al. Exosomes derived from tendon stem cells promote cell proliferation and migration through the TGF β signal pathway[J]. Biochem Biophys Res Commun, 2021, 536: 88-94.

[24] WANG S W, JU T Y, WANG J J, et al. Migration of BEAS-2B cells enhanced by H1299 cell derived-exosomes[J]. Micron, 2021, 143: 103001.

[25] SHARIATI NAJAFABADI S, AMIRPOUR N, AMINI S, et al. Human adipose derived stem cell exosomes enhance the neural differentiation of PC12 cells[J]. Mol Biol Rep, 2021, 48(6): 5033-5043.

[26] YANG S D, GUO S, TONG S, et al. Promoting osteogenic differentiation of human adipose-derived stem cells by altering the expression of exosomal miRNA[J]. Stem Cells Int, 2019, 2019: 1351860.

[27] ZHANG B B, ZHAXI D W, LI C, et al. M2 macrophagy-derived exosomal miRNA-26a-5p induces osteogenic differentiation of bone mesenchymal stem cells[J]. J Orthop Surg Res, 2022, 17(1): 137.

[28] WEN X, HU G, XIAO X, et al. FGF2 positively regulates osteoclastogenesis *via* activating the ERK-CREB pathway[J]. Arch Biochem Biophys, 2022, 727: 109348.

[29] ZHU G C, CHEN W, TANG C Y, et al. Knockout and double knockout of cathepsin K and *Mmp9* reveals a novel function of cathepsin K as a regulator of osteoclast gene expression and bone homeostasis[J]. Int J Biol Sci, 2022, 18(14): 5522-5538.

[30] HE F T, LUO S H, LIU S J, et al. *Zanthoxylum bungeanum* seed oil inhibits RANKL-induced osteoclastogenesis by suppressing ERK/c-JUN/NFATc1 pathway and regulating cell cycle arrest in RAW264. 7 cells[J]. J Ethnopharmacol, 2022, 289: 115094.

[31] KUMAR A, HUGHES T M, CRAFT S, et al. A novel approach to isolate brain-cell-derived exosomes from plasma to better understand pathogenesis of Alzheimer's disease[J]. Alzheimer's Dement, 2020, 16(Suppl 4): e044894.

[32] LI K, WONG D K, HONG K Y, et al. Cushioned-density gradient ultracentrifugation (C-DGUC): a refined and high performance method for the isolation, characterization, and use of exosomes[J]. Methods Mol Biol, 2018, 1740: 69-83.

[33] HELWA I, CAI J W, DREWRY M D, et al. A comparative study of serum exosome isolation using differential ultracentrifugation and three commercial reagents[J]. PLoS One, 2017, 12(1): e0170628.

[34] DING M, WANG C, LU X L, et al. Comparison of commercial exosome isolation kits for circulating exosomal microRNA profiling[J]. Anal Bioanal Chem, 2018, 410(16): 3805-3814.

[35] LIANG B, BURLEY G, LIN S, et al. Osteoporosis pathogenesis and treatment: existing and emerging avenues[J]. Cell Mol Biol Lett, 2022, 27(1): 72.

[36] LI K, XIU C M, ZHOU Q, et al. A dual role of cholesterol in osteogenic differentiation of bone marrow stromal cells[J]. J Cell Physiol, 2019, 234(3): 2058-2066.

[37] CHE Y T, YANG J Z, TANG F, et al. New function of cholesterol oxidation products involved in osteoporosis pathogenesis[J]. Int J Mol Sci, 2022, 23(4): 2020.

[38] LI K Q, CHEN S H, CAI P Y, et al. MiRNA-483-5p is involved in the pathogenesis of osteoporosis by promoting osteoclast differentiation[J]. Mol Cell Probes, 2020, 49: 101479.

[39] PARK E, LEE C G, LIM E, et al. Osteoprotective effects of loganic acid on osteoblastic and osteoclastic cells and osteoporosis-induced mice[J]. Int J Mol Sci, 2020, 22(1): 233.

[40] LAI G H, ZHAO R L, ZHUANG W D, et al. BMSC-derived exosomal miR-27a-3p and miR-196b-5p regulate bone remodeling in ovariectomized rats[J]. PeerJ, 2022, 10: e13744.

[41] SONG H Y, LI X Q, ZHAO Z C, et al. Reversal of osteoporotic activity by endothelial cell-secreted bone targeting and biocompatible exosomes[J]. Nano Lett, 2019, 19(5): 3040-3048.

[42] CHEN X T, WAN Z, YANG L, et al. Exosomes derived from reparative M2-like macrophages prevent bone loss in murine periodontitis models *via IL-10* mRNA[J]. J Nanobiotechnology, 2022, 20(1): 110.

[43] ZHU L F, LI L, WANG X Q, et al. M1 macrophages regulate TLR4/AP1 *via* paracrine to promote alveolar bone destruction in periodontitis[J]. Oral Dis, 2019, 25(8): 1972-1982.

[44] LIANG B L, WANG H C, WU D, et al. Macrophage M1/M2 polarization dynamically adapts to changes in microenvironment and modulates alveolar bone remodeling after dental implantation[J]. J Leukoc Biol, 2021, 110(3): 433-447.

[45] SHI M S, WANG C, WANG Y L, et al. Deproteinized bovine bone matrix induces osteoblast differentiation *via* macrophage polarization [J]. J Biomed Mater Res A, 2018, 106(5): 1236-1246.

[46] SHI C, YUAN F, LI Z L, et al. MSN@IL-4 sustainingly mediates macrophagocyte M2 polarization and relieves osteoblast damage *via* NF- κB pathway-associated apoptosis[J]. Biomed Res Int, 2022, 2022: 2898729.

[47] Horibe K, Hara M, Nakamura H. M2-like macrophage infiltration and transforming growth factor- β secretion during socket healing process in mice[J]. Arch Oral Biol, 2021, 123: 105042.

[48] WANG X Y, JI Q B, HU W H, et al. Isobavachalcone prevents osteoporosis by suppressing activation of ERK and NF-κB pathways and M1 polarization of macrophages[J]. Int Immunopharmacol, 2021, 94: 107370.

[49] LI Z K, ZHU X D, XU R J, et al. Deacylcynaropicrin inhibits RANKL-induced osteoclastogenesis by inhibiting NF-κB and MAPK and promoting M2 polarization of macrophages[J]. Front Pharmacol, 2019, 10: 599.

[50] YAO M Y, CUI B, ZHANG W H, et al. Exosomal miR-21 secreted by IL-1β -primed-mesenchymal stem cells induces macrophage M2 polarization and ameliorates sepsis[J]. Life Sci, 2021, 264: 118658.

[51] MA J, CHEN L, ZHU X, et al. Mesenchymal stem cell-derived exosomal miR-21a-5p promotes M2 macrophage polarization and reduces macrophage infiltration to attenuate atherosclerosis[J]. Acta Biochim Biophys Sin (Shanghai), 2021, 53(9): 1227-1236.

[52] LI R, LI D Z, WANG H N, et al. Exosomes from adipose-derived stem cells regulate M1/M2 macrophage phenotypic polarization to promote bone healing *via* miR-451a/MIF[J]. Stem Cell Res Ther, 2022, 13(1): 149.

[53] LI R, ZHAO K C, RUAN Q, et al. Bone marrow mesenchymal stem cell-derived exosomal microRNA-124-3p attenuates neurological damage in spinal cord ischemia-reperfusion injury by downregulating Ern1 and promoting M2 macrophage polarization[J]. Arthritis Res Ther, 2020, 22(1): 75.

［本文编辑］ 翟麟平

学术快讯

上海交通大学医学院附属第一人民医院王宏林团队揭示成纤维细胞介导炎症性皮肤过度神经支配的新机制

2023年4月10日，上海交通大学医学院附属第一人民医院王宏林团队在*Nature Communications*在线发表题为*Tenascin C*$^{+}$ *papillary fibroblasts facilitate neuro-immune interaction in a mouse model of psoriasis*的研究论文。研究团队利用*Pdgfra*^{DreER}-tdTomato小鼠对皮肤中的成纤维细胞实现了可视化荧光标记谱系示踪，并利用单细胞测序对正常与类银屑病小鼠皮肤成纤维细胞亚群进行了系统分析，发现炎症诱导产生了一群具有显著神经调控特征的成纤维细胞亚群。该研究创新性地揭示了损伤/炎症诱导的乳突真皮成纤维细胞功能性亚群促进神经免疫相互作用与银屑病炎症微环境的形成，阐明了细胞外基质蛋白TNC（tenascin-C）促进炎症性神经轴突异常增生的具体机制，为慢性皮肤炎症局部免疫微环境重塑提供了全新视角和治疗策略。